Phosphorylation of the Ndc80 complex protein, HEC1, by Nek2 kinase modulates chromosome alignment and signaling of the spindle assembly checkpoint

Randy Wei, Bryan Ngo, Guikai Wu, and Wen-Hwa Lee
Department of Biological Chemistry, School of Medicine, University of California, Irvine, Irvine, CA 92697

ABSTRACT **The spindle assemble checkpoint (SAC) is critical for accurate chromosome segregation. Hec1 contributes to chromosome segregation in part by mediating SAC signaling and chromosome alignment. However, the molecular mechanism by which Hec1 modulates checkpoint signaling and alignment remains poorly understood. We found that Hec1 serine 165 (S165) is preferentially phosphorylated at kinetochores. Phosphorylated Hec1 serine 165 (pS165) specifically localized to kinetochores of misaligned chromosomes, showing a spatiotemporal distribution characteristic of SAC molecules. Expressing an RNA interference (RNAi)-resistant S165A mutant in Hec1-depleted cells permitted normal progression to metaphase, but accelerated the metaphase-to-anaphase transition. The S165A cells were defective in Mad1 and Mad2 localization to kinetochores, regardless of attachment status. These cells often entered anaphase with lagging chromosomes and elicited increased segregation errors and cell death. In contrast, expressing S165E mutant in Hec1-depleted cells triggered defective chromosome alignment and severe mitotic arrest associated with increased Mad1/Mad2 signals at prometaphase kinetochores. A small portion of S165E cells eventually bypassed the SAC but showed severe segregation errors. Nek2 is the primary kinase responsible for kinetochore pS165, while PP1 phosphatase may dephosphorylate pS165 during SAC silencing. Taken together, these results suggest that modifications of Hec1 S165 serve as an important mechanism in modulating SAC signaling and chromosome alignment.**

Monitoring Editor
Yixian Zheng
Carnegie Institution

Received: Jan 6, 2011
Revised: Jul 22, 2011
Accepted: Aug 1, 2011

INTRODUCTION

Hec1 (also called Ndc80) is a conserved mitotic regulator dedicated to ensuring faithful chromosome segregation and genome integrity. Hec1 overexpression has been observed in a variety of human cancers, and was found to associate with adverse clinical outcomes of primary breast cancers and cases with multiple cancers (Chen *et al.*, 1997; van't Veer *et al.*, 2002; Glinsky *et al.*, 2005). At the molecular level, Hec1 forms a dumbbell-like heterotetramer with Nuf2, Spc24, and Spc25 to form the Ndc80 complex, which is part of the broad KMN network consisting of KNL-1, Mis12 complex, and Ndc80 complex at the kinetochore (Cheeseman *et al.*, 2006). Spc24 and Spc25 dimerize and face inward toward the centromere, while Hec1 and Nuf2 dimerize and their globular domains and N-terminal tails face outward. Hec1 has a microtubule-binding activity at its N-terminal region (aa 1–196), which is negatively regulated by the mitotic kinase Aurora B for proper kinetochore-microtubule attachment (Cheeseman *et al.*, 2006; Guimaraes *et al.*, 2008; Miller *et al.*, 2008).

Importantly, substantial evidence indicated that Hec1 plays a positive role in the spindle assembly checkpoint (SAC) control. The SAC is a mechanism that ensures faithful chromosome segregation by monitoring the kinetochore-microtubule attachment. This checkpoint is highly conserved from yeast to higher eukaryotes; the basic units of the mammalian SAC machinery include several Mads

This article was published online ahead of print in MBoC in Press (http://www.molbiolcell.org/cgi/doi/10.1091/mbc.E11-01-0012) on August 10, 2011.

W.H.L. serves as a member of the Board of Directors, GeneTex. This arrangement has been reviewed and approved by University of California–Irvine Conflict of Interest Committee.

Address correspondence to: Guikai Wu (gwu@uci.edu) or Wen-Hwa Lee (whlee@uci.edu).

Abbreviations used: DAPI, 4′,6-diamidino-2-phenylindole; EDTA, ethylenediaminetetraacetic acid; EGTA, ethylene glycol tetraacetic acid; FBS, fetal bovine serum; GFP, green fluorescent protein; NEB, nuclear envelope breakdown; PMSF, phenylmethylsulfonyl fluoride; pS165, phospho-serine 165; RNAi, RNA interference; S165, serine 165; SAC, spindle assembly checkpoint; siRNA, small interfering RNA.

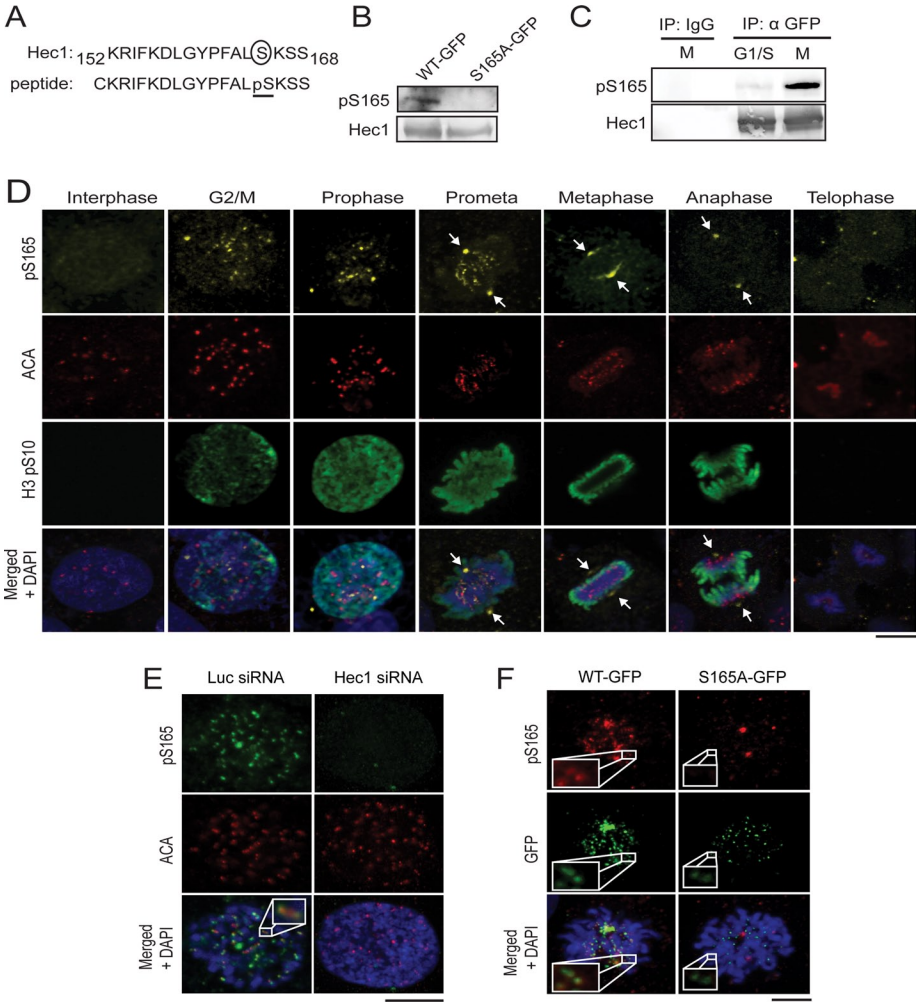

FIGURE 1: Generation of phospho-specific antibody recognizing Hec1 S165 phosphorylation during mitosis. (A) Diagram of Hec1 S165 phosphopeptide antigen used for generating phospho-specific antibody. (B) Western blot analysis of lysates from Hec1-WT-GFP– or Hec1-S165A-GFP–expressing cells using pS165 antibody. The same blot was stripped and reprobed with Hec1 (9G3) monoclonal antibody. (C) U2OS cells enriched at G1/S (double-thymidine block) or M phase (nocodazole), for which anti-pS165 antibody was used to blot immunoprecipitated Hec1-WT-GFP. The same blot was stripped and reprobed with anti-Hec1. (D) Unsynchronized MCF10A cells were stained with anti-pS165 (yellow), anti-centromere antibody (ACA; red), anti-Histone3 pSer10 antibodies (green), and DAPI (blue). Arrows indicate spindle poles. (E) Immunofluorescence staining with anti-pS165 (green) and ACAs (red) of U2OS cells transfected with Hec1 or luciferase siRNA. Inset image shows one pair of kinetochores. (F) pS165 staining is revealed in U2OS cells rescued with RNAi-resistant Hec1-WT-GFP, but not S165A mutant, when endogenous Hec1 is depleted. Insets show a pair of kinetochores. Scale bars: 5 μm.

(Mad1/Mad2), Bubs (Bub1/BubR1/Bub3), and Mps1 (Musacchio and Hardwick, 2002; Musacchio and Salmon, 2007). Unattached kinetochores recruit SAC components through a poorly understood mechanism, thereby eliciting a positive SAC signal to inhibit the anaphase-promoting complex/cyclosome necessary for sister chromatid separation and exit from mitosis (King *et al.*, 1995, 1996; Sudakin *et al.*, 1995). When cells are challenged with microtubule poisons to generate persistently unattached kinetochores, mitosis can be arrested for an average of 12 h in U2OS cells and 20 h in HeLa cells (Brito and Rieder, 2009). Active SAC signaling involves not only the above checkpoint effector molecules, but also structural components of the kinetochore and mitotic kinases (Musacchio and Salmon, 2007). For instance, the Ndc80 complexes are critical structural components of the kinetochore and are required for proper SAC control, as they recruit Mad1 and Mad2 to kinetochores (Martin-Lluesma *et al.*, 2002; DeLuca *et al.*, 2003; Buffin *et al.*, 2005; Lin *et al.*, 2006). Of disease relevance, overexpression of Hec1 in a transgenic mouse model caused high incidence of lung adenoma and hepatoma (Diaz-Rodriguez *et al.*, 2008), which correlated with SAC hyperactivation in mitotic cells. These animal studies reinforced previous observations that Hec1 (and the intact Ndc80 complex) is important for proper SAC control to prevent cancer-initiating chromosome missegregation.

During SAC signaling, Hec1 relays the checkpoint signals to downstream SAC effectors (Mad1 and Mad2). However, the exact regulation centered on Hec1 by upstream regulators is poorly understood. Proper SAC signaling is known to entail the delicate interplay of upstream mitotic kinases and phosphatases, aberrancy of which may undermine the accuracy of SAC control. It is therefore imperative to elucidate how Hec1 can be modulated by upstream kinases and phosphatases during SAC signaling. We have previously found that Hec1 is phosphorylated at serine 165 (S165) by the cancer-associated kinase Nek2 (Chen *et al.*, 2002). This phosphorylation site is conserved from yeast to human and is important for faithful chromosome segregation (Chen *et al.*, 2002; Du *et al.*, 2008). In this study, we sought to examine how this phosphorylation can contribute to faithful segregation, with the primary focus on the control of the SAC in the context of chromosome alignment.

RESULTS

To explore SAC signaling mediated by Hec1 phosphorylation at S165, we first raised a rabbit polyclonal antibody against Hec1 phospho-serine 165 (pS165) using a peptide antigen distinct from our previous design (Figure 1A; Chen *et al.*, 2002), in part because the previously used antibody is not suitable for immunofluorescence staining. For this study, the newly generated anti-pS165 antibody was affinity-purified and characterized. It recognized ectopically expressed wild-type (WT) Hec1 tagged with green fluorescent protein (GFP) but not the Hec1 S165A mutant (serine changed to alanine) in a Western blot assay (Figure 1B), suggesting that this antibody is specific to pS165. Consistently, the pS165 level was found to be much higher in cells enriched in mitotic phase than those at the G1/S phase (Figure 1C), confirming the previous observation (Chen *et al.*, 2002).

Phosphorylation of Hec1 is known to be cell cycle–dependent (Chen *et al.*, 2002). However, the details of steps in this process have yet to be explored. We examined the temporal and spatial distribution of pS165 in an immortalized noncancerous epithelial cell line, MCF10A. Notably, punctate pS165-staining signals were readily

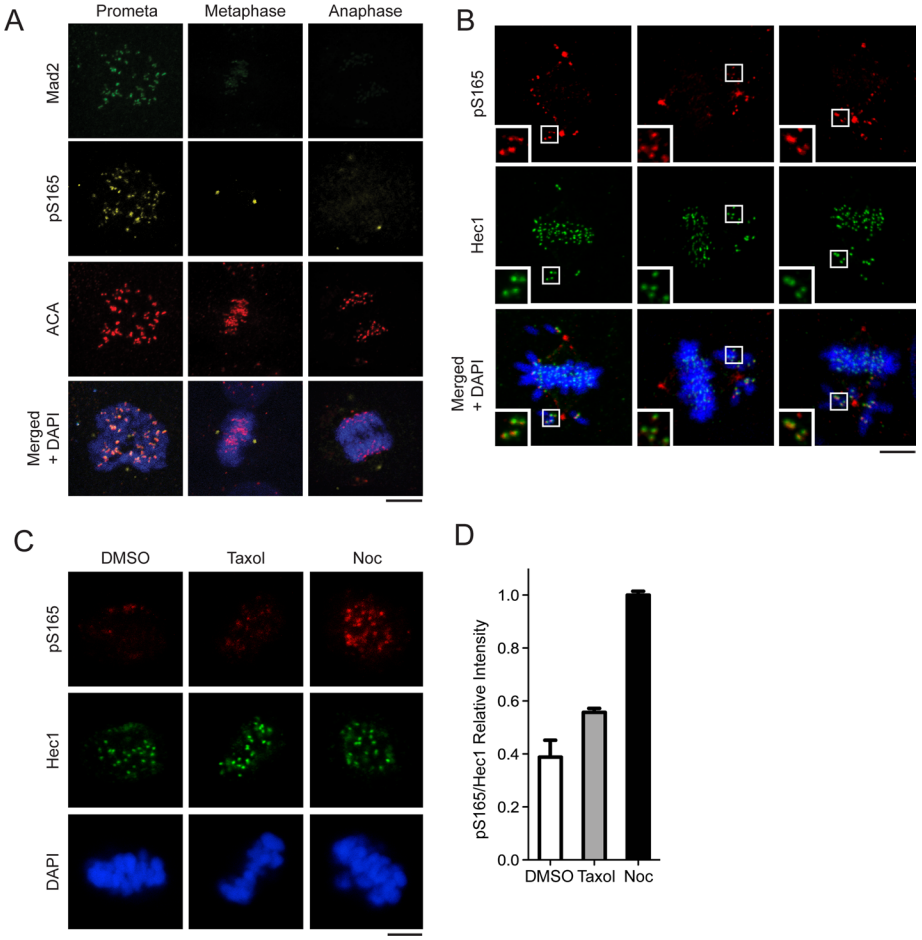

FIGURE 2: Phosphorylation of Hec1 S165 occurs specifically on kinetochores of misaligned chromosomes. (A) pS165 costaining with Mad2 in mitotic U2OS cells (prometaphase, metaphase, and anaphase). (B) pS165 costaining with Hec1 in mitotic MCF10A cells with misaligned chromosomes. Insets show magnified images of boxed regions. (C) pS165 costaining with Hec1 in U2OS cells arrested for 2 h with 10 μM MG132 prior to treatment with dimethyl sulfoxide (DMSO), Taxol (final concentration, 10 μM), or nocodazole (300 nM) for 1 h. (D) Relative fluorescence intensity of pS165 vs. total Hec1 in each cell population from (C) images (mean ± SEM; n > 200 kinetochores from seven individual cells). All images were captured under the same exposure settings. For all images, chromosomes were stained with DAPI (blue). Scale bars: 5 μm.

detected in mitotic cells, which colocalized with the kinetochore marker anti-centromere antibody (ACA; Figure 1D). Kinetochore pS165 signals were not evident in interphase cells but became detectable at the G2/M transition and peaked at prophase and prometaphase, eventually diminishing at metaphase and disappearing at later mitotic stages (Figure 1D), even though Hec1 is present at kinetochores during all stages of mitosis (Chen *et al.*, 1997). These kinetochore pS165 signals were abolished upon depletion of endogenous Hec1 by small interfering RNA (siRNA; Figure 1E). To ascertain that these punctate foci were endogenous pS165 signals, rather than nonspecific epitopes that can be masked by structural alteration of kinetochores upon Hec1 depletion, we complemented Hec1-depleted cells with an RNA interference (RNAi)-resistant WT Hec1 or the S165A (serine mutated to alanine) point mutant tagged with GFP. The WT Hec1, but not the S165A mutant, restored the kinetochore pS165 signal (Figure 1F). Taken together, these results validated that the anti-pS165 antibody is specific to Hec1 S165, and revealed that the kinetochore Hec1 is phosphorylated at this residue during the early stages of mitosis.

It was noticed that pS165 also showed clear distribution to spindle poles, where staining was reduced but not completely abolished after treatment with Hec1 siRNA (unpublished data). This is probably due to enhanced stability of centrosomal pS165 species because Hec1 is present at centrosomes to interact with Hice1 (Wu *et al.*, 2009), or nonspecific antibody cross-reactivity with a phospho-species at the centrosome.

Although pS165 signals were absent from kinetochores after metaphase, endogenous Hec1 persisted on these kinetochores (Supplemental Figure S1A). The same temporal and spatial distribution of pS165 signals was also observed in the kangaroo rat Ptk2 cells (Figure S1B). The pattern and timing of pS165 signals are reminiscent of SAC-signaling proteins. To test whether pS165 represents active SAC signaling, we costained U2OS mitotic cells with antibodies for pS165 and Mad2. We found that Mad2 colocalized with pS165 on kinetochores primarily at prophase and prometaphase, but not at metaphase or after onset of anaphase (Figure 2A). Further, because misaligned chromosomes often incur active SAC signaling, we examined the status of pS165 on misaligned chromosomes. The pS165 signals on kinetochores were preferentially retained on chromosomes that had not congressed to the middle plate but were absent from those that were already properly aligned (Figure 2B). Thus the kinetochore pS165 signal is characteristic of a marker of active SAC signaling. To gain further evidence to support this notion, we then tested whether the kinetochore pS165 can be retained or generated on metaphase chromosomes that have been intentionally perturbed to increase chromosome misalignment by using the spindle poison nocodazole or Taxol. For this purpose, U2OS cells were transiently arrested at metaphase by a proteosome inhibitor, MG132, and then treated with vehicle control, Taxol, or nocodazole (Nishino *et al.*, 2006; Elowe *et al.*, 2007; Huang *et al.*, 2008). Control-treated cells exhibited positive Hec1 but negative pS165 signal at metaphase kinetochores (Figure 2C). In comparison, nocodazole or Taxol treatment increased the kinetochore pS165 signal significantly (Figure 2C). It is noted that nocodazole treatment yielded kinetochore pS165 signals that were about twofold stronger than in the Taxol-treated group (Figure 2D), probably because pS165 is more responsive to loss of kinetochore-microtubule attachment than loss of tension caused by Taxol. Taken together, these results demonstrated that kinetochore pS165 represents active SAC signaling.

The correlation of kinetochore pS165 with SAC signaling suggested that S165 plays an active role in the SAC control. To explore this possibility, we expressed Hec1-GFP fusions (WT and S165A) as RNAi-resistant versions in U2OS cells via retroviral gene delivery. In the presence of endogenous Hec1, the integrated Hec1-GFP allowed fairly normal mitosis and cell proliferation for over 1 mo, suggesting minimal cytotoxicity. Importantly, the expression of

Hec1-GFP did not alter the expression levels of SAC proteins compared with uninfected parental cells (Figure S2), nor did the expression of Hec1 WT versus S165A mutant when cells were treated with Hec1 siRNA (resultant cells are hereafter called WT cells and S165A cells in all figures, respectively; Figure 3A). The expression of Hec1 WT or S165A mutant alone did not significantly change the mitotic index of parental cells (Figure 3B). Knockdown of endogenous Hec1 alone increased the mitotic index to a level (31%) comparable to that of the previous study (Martin-Lluesma *et al.*, 2002). Notably, in Hec1 knockdown cells, expressing Hec1 WT or S165A mutant restored the mitotic index almost to the parental level (Figure 3B).

To pinpoint whether S165A might affect the SAC activity of cells, we examined the mitotic progression of WT and S165A cells using time-lapse microscopy (Figure 3C). The initial time point was zeroed at nuclear envelope breakdown (NEB) and the duration from NEB to anaphase onset was measured (Figure 3D). The duration from NEB to anaphase onset averaged 57 ± 3 min for WT cells (n = 23) but was shorter for S165A cells (42 ± 2 min; n = 36; $p < 0.001$; Figure 3D). To determine whether the decrease in NEB-to-anaphase onset time was due to faster chromosome alignment or premature anaphase entry, we reexamined the time-lapse recordings to measure the duration from 1) NEB to metaphase and 2) metaphase to anaphase. The WT and S165A cells had a similar duration from NEB to metaphase, but S165A cells had a shorter metaphase-to-anaphase transition (Figure 3E). These observations suggested that S165A did not alter the duration of chromosome alignment, but promoted precocious anaphase entry, probably due to defective SAC.

To further examine SAC activity, we challenged cells with 50 ng/ml nocodazole to create unattached kinetochores, thereby enhancing SAC response. The mitotic indices were then calculated at indicated time points. Measurement of the kinetics of mitotic indices upon nocodazole treatment showed that both WT and S165A cells were initially delayed in mitosis (Figure 3F). However, the mitotic index of S165A cells peaked at only ~41%, significantly lower than that of WT cells (~60%; $p < 0.001$). This result suggested a weakened SAC in the S165A cells. It is noteworthy that the reduction of mitotic index of WT and S165A cells after 20 h was not likely to be due to cell death; this became apparent only after 48 h. Because S165 is located in the CH domain of Hec1, our results supported the previous observation that the CH domain is involved in SAC control (Ciferri *et al.*, 2008).

To confirm that S165A indeed weakens the SAC, we assessed SAC activity using time-lapse microscopy of cells stressed with nocodazole treatment. Intriguingly, when cells were treated with nocodazole (20 or 100 ng/ml), the mitotic durations of WT and S165A cells differed more with a higher dosage of the drug. At the dosage of 20 ng/ml, the duration was 194 ± 9 min for WT cells (n = 58) and 72 ± 6 min for S165A cells (n = 44; $p < 0.001$; Figure 3G). At 100 ng/ml, the duration of WT cells (n = 18) was increased to 311 ± 18 min, whereas that of S165A cells (n = 22) was only increased to 95 ± 14 min ($p < 0.001$). These findings argued strongly for a weakened SAC in S165A cells. Notably, these S165A cells, similar to other cells defective in several known SAC molecules (Burds *et al.*, 2005; Kienitz *et al.*, 2005), showed more frequent lagging chromosomes during anaphase than WT cells (Figure 3H), and consequently, higher incidences of micronuclei, multinuclei, and dead cells (Figure 3, I–J). Taken together, the results highlighted a critical role of S165 for adequate SAC activity. The results also suggested that the shortening of mitotic duration in S165A cells was not attributable to more rapid chromosome movement.

The SAC machinery is composed of multiple effectors that are specifically recruited to unattached kinetochores to relay an inhibitory signal to delay anaphase onset. Thus it is likely that the phosphorylation at Hec1 S165 may affect SAC effector molecules. To test this possibility, we performed immunofluorescence staining using a set of antibodies specific for key SAC molecules (including Mad1, Mad2, ZW10, Zwint-1, and BubR1). We quantified the intensity of SAC proteins at the prometaphase kinetochores against that of ACA. Importantly, Mad1 and Mad2 were reduced by 65 and 50%, respectively, in S165A cells compared with WT cells (Figure 4F). The reduction of Mad1 and Mad2 was not a result of decreased protein level, since the expression of all SAC components was unaltered by S165A (Figure 3A). Furthermore, the kinetochore Mad1/Mad2 signals were properly retained on misaligned metaphase chromosomes in WT cells, but were significantly diminished in S165A cells (Figure 4, G and H). Taken together, these results suggest that phosphorylation of S165 is important for Mad1/Mad2 localization at kinetochores for active SAC signaling. However, how S165 phosphorylation triggers Mad1/Mad2 recruitment to the kinetochore is unclear. Others and we have not been able to demonstrate direct binding between Mad1 (or Mad2) and Hec1, and thus we believe that the Mad1/Mad2 recruitment to kinetochores probably requires additional factors (Martin-Lluesma *et al.*, 2002).

Following the phosphorylation of S165 during earlier stages of mitosis, the kinetochore pS165 signal diminished after metaphase alignment and prior to anaphase onset (Figure 1E), correlating with the timing of proper attachment of microtubules to kinetochores. We reasoned that pS165 has to be removed to allow timely anaphase entry; failure to remove pS165 would lead to robust SAC signaling. To test this idea, we generated an RNAi-resistant and phosphomimic Hec1 S165E (S165 changed to glutamate) retrovirus. As for S165A, retroviral expression of S165E mutant did not alter the level of SAC proteins compared with WT, nor did protein levels change following depletion of endogenous Hec1 (Figure 5A). Intriguingly, the expression of S165E alone in U2OS cells caused a threefold increase of mitotic index (Figure 5B) and prometaphase enrichment (~70% of mitotic cells) after 48 h of expression, indicative of a dominant negative effect to trigger SAC activation. When cells were concomitantly depleted of endogenous Hec1 (resultant cells are hereafter called S165E cells), the mitotic index increased further (sevenfold; Figure 5B). To further dissect the mitotic phenotypes of S165E cells, we performed time-lapse imaging of individual live cells in the absence of spindle poisons. Live-cell imaging demonstrated that S165E cells depleted of endogenous Hec1 were dramatically delayed at prometaphase (Figure 5C). For these cells, the duration from NEB to anaphase onset was significantly longer (208 ± 19 min; n = 25) than the WT control (57 ± 3 min; n = 23; Figure 5D). When the S165E cells were challenged with nocodazole (50 ng/ml), the mitotic indices were significantly higher than those of WT cells at early time points (Figure 5E), but the differences were negligible at later time points (12 h or later; Figure 5E).

The mitotic effects of S165E cells appeared not to be the simple opposite of those of S165A cells, but rather suggested a major defect in chromosome alignment. Consistent with this notion, none of the S165E cells (0 of 2000 fixed mitotic cells) could form a distinct metaphase plate. A few did bypass the SAC (47 of 2000), of which over one-half (28 of 47) showed anaphase lagging chromosomes (Figure 5F), eventually leading to massive segregation errors indicated by high levels of micronuclei, multinuclei, and consequential cell death (Figure 5G). Apparently, the major defect of chromosome alignment caused by S165E has masked the direct effect of this mutant in SAC signaling. Nevertheless, the prometaphase S165E cells showed higher intensity of Mad2 and Mad1 kinetochore foci than the WT control (Figure 5H), indicating a robust

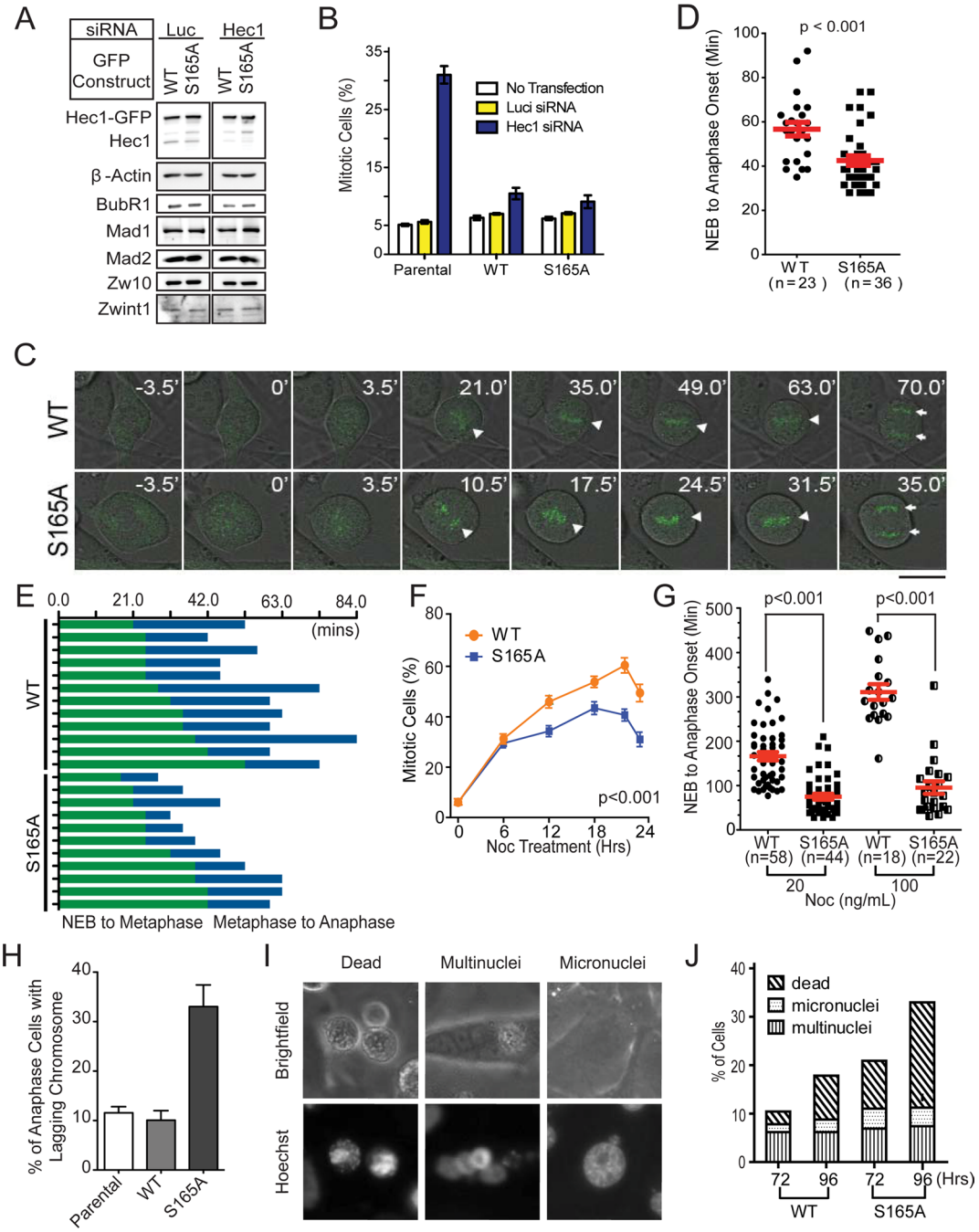

FIGURE 3: Expression of Hec1 S165A results in shortened mitotic duration and increased chromosomal segregation errors. (A) Western blot analysis of Hec1-depleted cells expressing RNAi-resistant Hec1-WT-GFP or Hec1-S165A-GFP. Luciferase siRNA was used as a control. The expressions of BubR1, Mad1, Mad2, Zw10, and Zwint1 were also examined. β-Actin served as an internal loading control. (B) Mitotic index of U2OS parental cells and U2OS cells ectopically expressing RNAi-resistant Hec1-WT-GFP or Hec1-S165A-GFP. Cells were either transfected with luciferase or Hec1 siRNA, or not transfected at all. About 1000 cells were collected for each sample from two separate experiments. (C) Time-lapse microscopy of WT and S165A cell during mitosis. Images were captured at 3.5-min intervals. Triangles indicate chromosomes aligned along the metaphase plate. Arrows indicate separated sister chromatids. Scale bar: 10 μm. (D) Quantification of time from NEB to anaphase onset in WT and S165A cells without nocodazole. (E) Duration of time that WT or S165A cells were undergoing NEB-to-metaphase onset and metaphase-to-anaphase onset. (F) Percentage of mitotic cells expressing WT or S165A mutant after depletion of the endogenous Hec1 and treatment with 50 ng/ml nocodazole. Cells were randomly photographed at the designated time point using fluorescence and phase-contrast microscopy. About 500 cells were collected for each sample and time point. (G) Quantification of time from NEB-to-anaphase onset in WT and S165A cells with 20 or 100 ng/ml of nocodazole. (mean ± SEM; images of cells collected from two independent experiments; $p < 0.001$). (H) Percentage of WT or S165A cells with lagging chromosomes during anaphase 48 h after Hec1 siRNA transfection. (I) Representative images of interphase nuclei stained with Hoechst 33342 (top) and their corresponding bright field images (bottom). Scale bar: 10 μm. (J) Quantification of multinucleated, micronucleated, and dead cells 72 and 96 h after depletion of endogenous Hec1 with siRNA (mean ± SEM; $n > 400$ cells per sample).

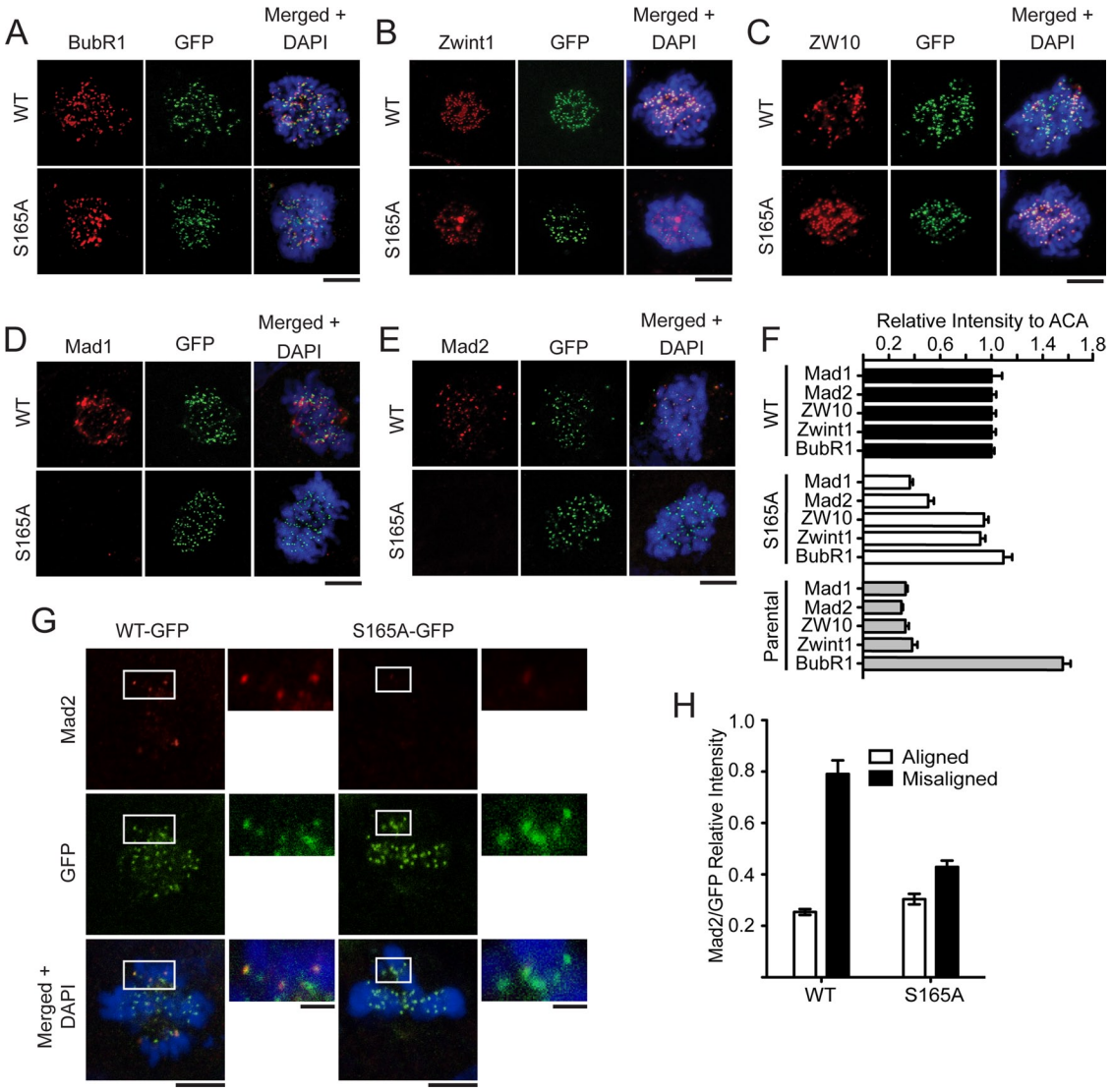

FIGURE 4: Expression of Hec1 S165A impairs recruitment of Mad1 and Mad2 to kinetochores. (A–E) WT and S165A cells were immunostained with antibodies against BubR1 (A), Zwint1 (B), ZW10 (C), Mad1 (D), and Mad2 (E) after depletion of endogenous Hec1. Scale bar: 5 μm. (F) Quantification of SAC-staining intensities at kinetochores (normalized for ACA staining; mean ± SEM; n > 150 kinetochores from 10 different cells). (G) Mad2 staining in U2OS cells rescued with Hec1-WT-GFP or the S165A mutant when endogenous Hec1 is depleted. Insets show magnified images of boxed regions. (H) Quantification of Mad2 fluorescence intensity on aligned and misaligned chromosomes. For all images, chromosomes were stained with DAPI (blue). Scale bars: 5 μm.

SAC response. Taken together, these results suggested that the S165E mutant hampered chromosome alignment, which in part ignited a robust SAC signaling to prevent timely anaphase entry.

To address how S165E may mechanically affect the chromosome alignment, we tested whether it affects the k-fiber (kinetochore microtubules) stability using a cold-stability assay. We found that S165E cells had less cold-stable kinetochore microtubules than WT or S165A cells (Figure S3), suggesting that reduced k-fiber stability may account for the defect in chromosome alignment. It is possible that the S165E mutation may trigger a structural change more profound than phosphorylation and affect the microtubule-binding by Hec1, as suggested in a previous study (Lou *et al.*, 2004).

Nek2 is the mitotic kinase known to directly phosphorylate Hec1 at S165 for faithful chromosome segregation (Chen *et al.*, 2002). Knockdown of Nek2 impairs Mad2 localization at kinetochores and negatively affects the SAC (Lou *et al.*, 2004). Therefore Nek2 is a candidate upstream kinase responsible for generating pS165 signals on kinetochores. In mammalian cells, Nek2 has two major isoforms (Nek2A and Nek2B). Nek2A is substantially degraded at prometaphase, whereas Nek2B is sustained throughout mitosis. Both isoforms, either one of which may be sufficient for generating pS165 signals, were associated with Hec1 in a coimmunoprecipitation assay (Figure 6A). Consistently, Nek2 knockdown by siRNA significantly reduced the kinetochore pS165 signal (> 70% reduction; Figure 6, B and C). Furthermore, endogenous Nek2 was found to colocalize with the pS165 signal at kinetochores (Figure 6D), suggesting possible on-site phosphorylation at kinetochores by Nek2. On the other hand, in budding yeast, the checkpoint kinase Mps1 was shown to phosphorylate Ndc80 (yeast Hec1), therefore affecting SAC activation; however, treating human cells with potent Mps1 inhibitors (MPS-IN-1) had no evident effect on kinetochore pS165 signals (Figure S4, A and B), arguing against

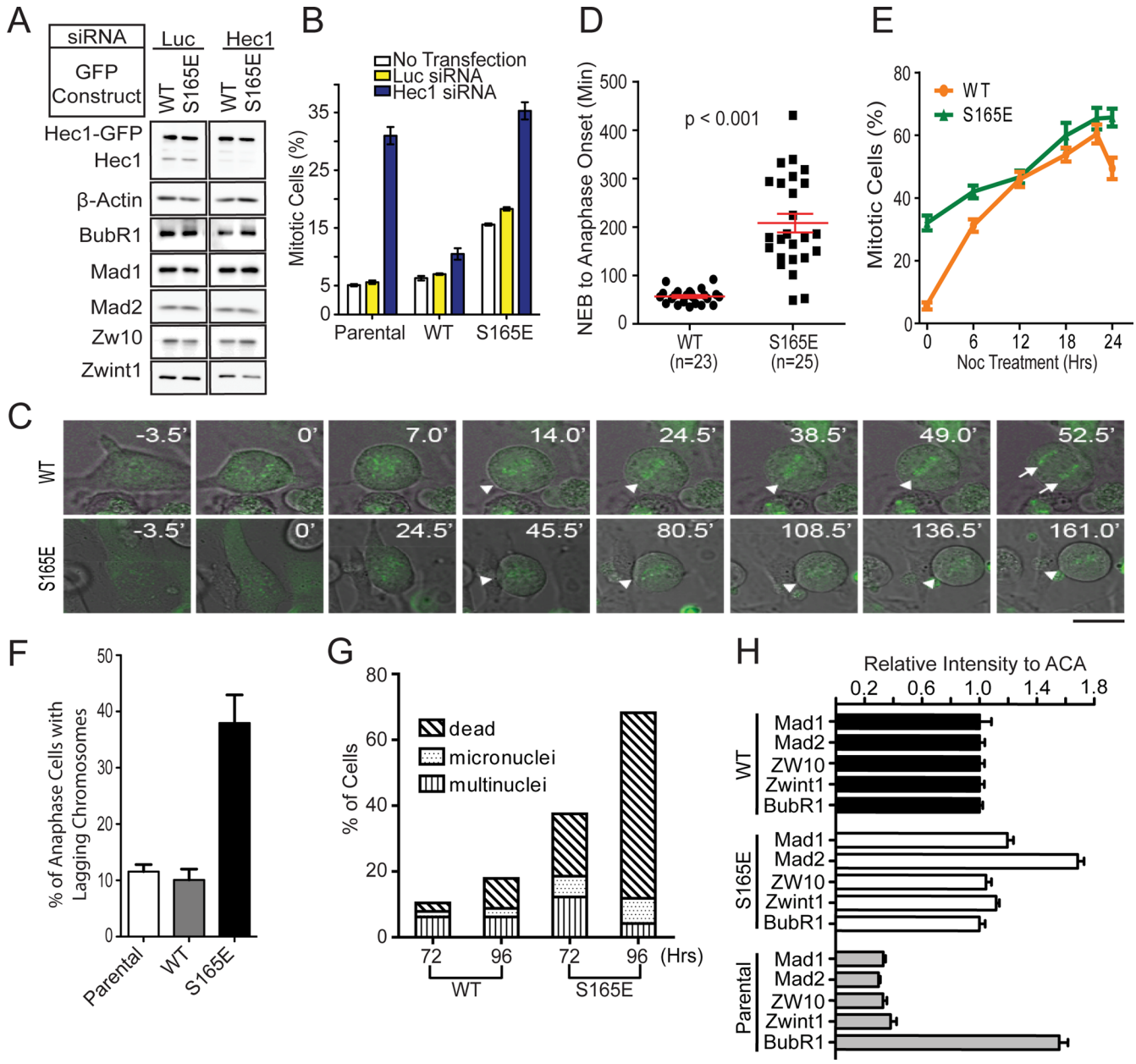

FIGURE 5: Expression of Hec1 S165E prolongs mitotic duration, increases segregation errors, and causes cell death. (A) Western blot analysis of Hec1-depleted cells expressing RNAi-resistant Hec1-WT-GFP or Hec1-S165E-GFP. Luciferase siRNA was used as a control. The expressions of BubR1, Mad1, Mad2, Zw10, and Zwint1 were also examined with their specific antibodies. β-actin served as a loading control. (B) Mitotic index of U2OS parental cells and U2OS cells ectopically expressing RNAi-resistant Hec1-WT-GFP or Hec1-S165E-GFP. Cells were either transfected with luciferase or Hec1 siRNA, or untransfected. About 1000 cells were collected for each sample from two separate experiments. (C) Time-lapse microscopy of WT and S165E cell during mitosis. Images were captured at 3.5-min intervals. Triangles indicate chromosomes aligned along the metaphase plate. Arrows indicate separated sister chromatids. Scale bar: 10 μm. (D) Quantification of time from NEB-to-anaphase onset of WT and S165E cells without nocodazole. (mean ± SEM; images collected from two independent experiments; $p < 0.001$). (E) Percentage of mitotic cells expressing WT or S165E mutant after depletion of the endogenous Hec1 with siRNA and subsequent treatment with 50 ng/ml nocodazole. Cells were randomly photographed at the designated time point using fluorescence and phase-contrast microscopy. About 500 cells were collected for each sample and time point. (F) Percentage of WT or S165A cells with lagging chromosomes during anaphase 48 h after Hec1 siRNA transfection. (G) Quantification of multinucleated, micronucleated, and dead cells 72 and 96 h after depletion of endogenous Hec1 (mean ± SEM; $n > 400$ cells per sample). (H) Quantification of SAC-staining intensities at kinetochores (normalized for ACA staining; mean ± SEM; $n > 150$ kinetochores from 10 different cells).

the role of Mps1 in generation of pS165 in mammalian cells. Taken together, these results suggested that Nek2 may serve as a primary upstream kinase in generation of pS165 during SAC signaling.

Active SAC signaling has to be silenced to permit timely anaphase onset. The pS165 signals diminished at metaphase kinetochores when chromosomes had achieved proper alignment,

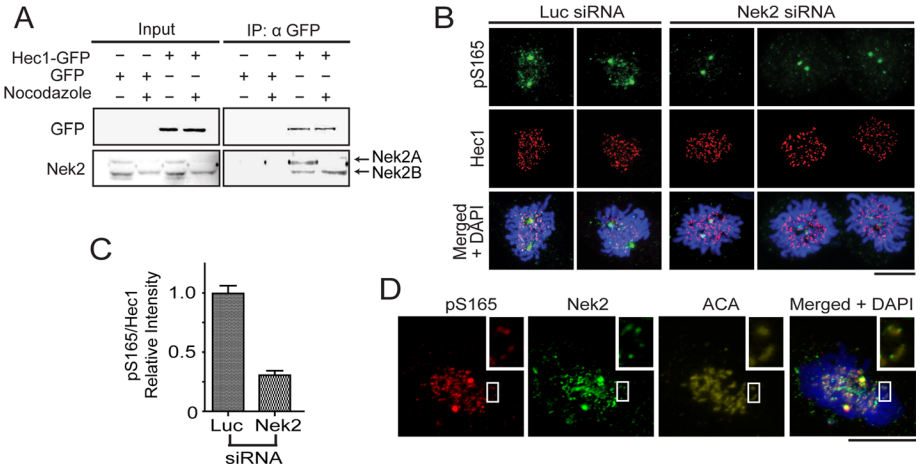

FIGURE 6: Nek2 phosphorylates Hec1 on S165. (A) In untreated GFP and Hec1-WT–expressing U2OS cells, Nek2A and Nek2B are expressed at comparable levels, and coimmunoprecipitation of Hec1-WT pulled down both Nek2A and Nek2B. On nocodazole treatment, Nek2A but not Nek2B levels were reduced, and only Nek2B coimmunoprecipitated with Hec1-WT. (B) pS165 staining is present in U2OS cells transfected with luciferase siRNA, but not when transfected with Nek2 siRNA. Cells were stained with anti-pS165 (red), anti-Hec1 antibodies (green), and DAPI (blue). (C) Quantification of pS165-staining intensities at kinetochores (normalized for total Hec1) in luciferase or Nek2 siRNA-treated U2OS cells (mean ± SEM; n > 200 kinetochores from seven individual cells.) All images were captured under the same exposure settings. (D) Nek2 and pS165 colocalized at kinetochores of U2OS cells. Cells were costained with anti-pS165 (red) and anti-Nek2 antibodies (green), anti-ACA (yellow), and DAPI (blue). Inset is higher magnification image of boxed region. Scale bars: 5 μm.

correlating with checkpoint silencing. The removal of pS165 was not attributed to Hec1 degradation, because endogenous Hec1 persisted on the pS165-negative kinetochores, such as those at anaphase or telophase (Figure S1A). Rather, a phosphatase is likely to be responsible for dephosphorylating pS165 during checkpoint silencing. Both PP1 (PP1α and -β) and PP2A are known to localize to the kinetochore, where they play important regulatory roles (Gentry and Hallberg, 2002; Trinkle-Mulcahy *et al.*, 2006; Kim *et al.*, 2010; Liu *et al.*, 2010). PP1 is required for silencing the SAC in yeast, but its exact downstream targets are not known (Pinsky *et al.*, 2009; Vanoosthuyse and Hardwick, 2009). Initially, the pS165 signals were barely detectable unless the phosphatase inhibitor Microcystin-LR was added to the extraction buffer before fixation, which is a potent inhibitor for the serine/threonine phosphatases PP1 and PP2A. To further determine whether PP1 or PP2A is responsible for dephosphorylating pS165, we tested two additional PP1 and PP2A inhibitors (okadaic acid and calyculin A) and one PP2A-specific inhibitor, fostriecin (10,000-fold selectivity for PP2A over PP1) during the prefixation extraction step in MCF10A (Figure 7A), U2OS, and Ptk2 cell lines (Figure S5, A and B). At 500 nM, all three PP1 and PP2A inhibitors (okadaic acid, Microcystin-LR, and calyculin A) were able to preserve kinetochore pS165 signals in all three cell lines; Microcystin-LR did so even at a much lower concentration (100 nM), while the PP2A-specific inhibitor fostriecin failed to preserve pS165 at either concentration (Figures 7A and S5, A and B), suggesting that PP1 may be responsible for dephosphorylation of pS165. Consistently, a portion of cellular PP1 was found to associate with Hec1 in a coimmunoprecipitation assay (Figure 7B); this association is perhaps mediated by KNL1 in the context of KMN networking, which directly interacts with PP1 via a defined motif (Liu *et al.*, 2010). Furthermore, treating cells with the PP1 inhibitor (okadaic acid), but not the PP2A inhibitor (fostriecin), resulted in a mitotic accumulation at the prophase and prometaphase stages (Figure 7, C and D), reflective of active SAC signaling when PP1 was inactivated. Although direct enzymatic evidence is not available, these results implicate PP1 in pS165 dephosphorylation that facilitates SAC silencing.

DISCUSSION

In this study, we identified a novel SAC-signaling module centered on Hec1 S165 within the N-terminal region. S165 appears to serve as an intricate molecular switch modulating the activity of the SAC. Lack of S165 phosphorylation weakens the SAC, in part by reducing the Mad1/Mad2 signals at kinetochores. During early mitotic stages, pS165 preferentially localizes to kinetochores on misaligned chromosomes, which often lack microtubule attachment. On successful chromosome alignment, pS165 is dephosphorylated to allow timely anaphase entry. The spatial and temporal distribution of pS165 is typical of a SAC marker such as the 3F3/2 phospho-epitope (Gorbsky and Ricketts, 1993; Campbell and Gorbsky, 1995; Wong and Fang, 2007).

The role of S165 in SAC signaling seems to be delicate, yet critically important for faithful chromosome segregation. It specifically fortifies the Mad2/Mad1 signals at the kinetochore. The results concur with and further deepen the previous understanding that Hec1 is required for proper Mad2 localization to kinetochores (Martin-Lluesma *et al.*, 2002). How is this delicate control achieved at the molecular level? It has been shown that Mad2 preferentially recognizes phosphorylated kinetochores (Waters *et al.*, 1999). Yet evidence for direct interaction between Hec1 and Mad2 (or Mad1) is lacking. It is possible that S165, in response to signaling from upstream kinases, becomes phosphorylated as an integral part of an unspecified multicomponent module that recruits Mad1 and Mad2. This unspecified module presumably includes the checkpoint kinase Mps1, because it dictates the Mad2 signaling at kinetochores (Tighe *et al.*, 2008; Hewitt *et al.*, 2010; Kwiatkowski *et al.*, 2010; Sliedrecht *et al.*, 2010), and requires Hec1 for its own kinetochore localization and early activation (Saurin *et al.*, 2011). Yeast Mps1 was shown to interact with the N-terminal region of Ndc80. It was therefore intriguing to test whether S165 may facilitate Mps1 localization and activation at the kinetochores during early mitosis of mammalian cells. On the other hand, Mps1 can directly phosphorylate Hec1 in a feedback manner, at least in yeast (Kemmler *et al.*, 2009). Using potent Mps1 inhibitors, we have shown that S165 is not the target site for mammalian Mps1 (Figure S4). Another possible scenario is that phosphorylation of S165 is an early SAC activation step that precedes and potentiates the Mps1-mediated phosphorylation on other residues, which together with pS165 allow full activation of the Hec1-Mps1-Mad2 signaling cascade.

Hec1 is becoming increasingly prominent as a potential link between microtubule binding and checkpoint control. The N-terminal tail of Hec1 is a major part of the KMN network that constitutes several sites for microtubule attachment. Aurora B is the critical kinase that phosphorylates this N-terminal tail to release faulty attachments and ensures proper chromosome biorientation and alignment (Cheeseman *et al.*, 2006; DeLuca *et al.*, 2006); Aurora B has also recently been shown to act together with Hec1 to ensure early

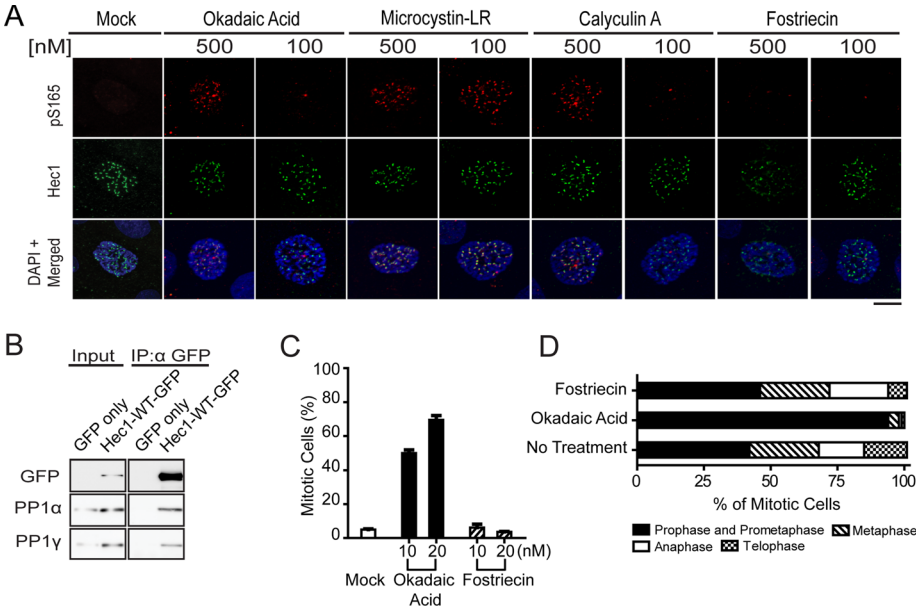

FIGURE 7: Inhibition of PP1 phosphatase preserves Hec1 pS165 signal. (A) MCF10A cells were immunostained with anti-pS165 antibodies (red) and anti-Hec1 (9G3), antibodies (green), using prefixation extraction buffer containing either 500 nM or 100 nM of specific phosphatase inhibitor or mock inhibitor (DMSO). Cells were counterstained with DAPI (blue). Scale bar: 5 μm. (B) Ectopically expressed Hec1-WT-GFP was coimmunoprecipitated with endogenous PP1α and PP1γ by anti-GFP antibody. (C) Mitotic index of U2OS cells treated for 18 h with 10 or 20 nM of either okadaic acid or fostriecin. About 1000 cells were collected for each sample from two separate experiments. (D) Mitotic distribution of different stages of U2OS cells following treatment with 20 nM okadaic acid or 20 nM fostriecin for 18 h.

SAC activation (Saurin *et al.*, 2011). Because S165 is physically close to the N-terminal tail, it may conveniently convey the status of microtubule attachment to downstream SAC effectors. Our unpublished data suggested that Aurora B affects the status of pS165 and Nek2, thus providing initial evidence pointing toward a possible Aurora B-Nek2-Hec1 signaling branch of the SAC. Meanwhile, possibly due to the close proximity of S165 to the N-terminal tail, the serine to glutamate change (S165E) seemed to cause significant effects both in chromosome alignment and SAC signaling (Figure 5). In this regard, it is noted that S165 is within the microtubule-binding "toe" of the Hec1 CH domain and is close to a few key residues, including K166 (Alushin *et al.*). Conceivably, phosphorylation of S165 may dislodge K166 from the microtubule lattice and hence be recognized as an indicator of detachment or a signal of SAC activation.

Our study suggests that Nek2 and PP1 are the candidate antagonistic pair of enzymes for modifying S165 in a dynamically sequential manner. Nek2 is prominent for its roles in centrosome duplication and separation (Hayward and Fry, 2006; O'Regan *et al.*, 2007). The novel role of Nek2 in SAC signaling can be direct, because a portion of Nek2 is located at the kinetochore, as shown by this study and others (Lou *et al.* 2004). The timing and mode of action by Nek2 must be carefully examined, since two Nek2 isoforms may function during mitosis, Nek2A and Nek2B (Uto *et al.*, 1999; Hames and Fry, 2002). Nek2A is degraded during mitosis, starting at prometaphase, in an APC-dependent manner, whereas Nek2B, a C-terminal splice variant of Nek2A, persists throughout mitosis (Hames *et al.*, 2001; Hames and Fry, 2002; Hayes *et al.*, 2006). One relevant question is how the pS165 signal is maintained on the misaligned kinetochores at metaphase, during which Nek2A is presumably already downregulated. Both Nek2A and Nek2B can be associated with Hec1 (Figure 6). Thus Nek2B or, less possibly, an unknown substitute kinase, may target S165 to sustain SAC signaling when Nek2A becomes substantially degraded. Of clinical relevance, the Nek2-Hec1 node of mitotic network has now been exploited as a promising target of cancer therapeutic inhibitors (Wu *et al.*, 2008).

The role of PP1 in SAC silencing is well documented, but its downstream targets are poorly understood. Using phosphatase inhibitors, we observed that PP1 may be responsible for the dephosphorylation of Hec1 pS165. Since a portion of cellular PP1 can be coimmunoprecipitated with Hec1, a close interaction between these two exists. PP1 directly binds KNL-1 via a conserved PP1-interacting motif (Liu *et al.*, 2010) that, together with Hec1, is a part of the KMN network. Alternatively, PP1 has been shown to interact directly with Nek2 (Helps *et al.*, 2000), which binds to Hec1 directly (Chen *et al.*, 2002). In either situation, Hec1 is closely associated with PP1. Although direct evidence to support the enzyme–substrate relationship between PP1 and Hec1 is currently unavailable, the circumstantial evidence described herein implicates PP1, but not PP2, as the enzyme that dephosphorylates pS165. Whether the dephosphorylation of pS165 of Hec1 is executed in the complex of KMN or Nek2/PP1 remains to be explored.

MATERIALS AND METHODS

Cell culture and RNAi

Human osteosarcoma cell line U2OS was cultured in DMEM supplemented with 10% heat-inactivated fetal bovine serum (FBS) at 37°C under 10% CO_2. MCF10A cell line was cultured in DMEM/F12 (50:50), supplemented with 5% horse serum, 0.1 μg/ml cholera toxin, 10 μg/ml insulin, 0.5 μg/ml hydrocortisone, and 20 ng/ml epidermal growth factor. Ptk2 cell line was cultured in Advanced MEM (Invitrogen, Carlsbad, CA) supplemented with 10% FBS. siRNA duplexes previously validated to target Hec1 and Nek2 were custom-synthesized by Ambion (Austin, TX; Martin-Lluesma *et al.*, 2002). Cells were transfected twice within 24 h using Lipofectamine 2000 according to the manufacturer's instructions (Invitrogen). Twenty-four hours after the last siRNA transfection, cells were used for experiments or lysed for Western blot analysis.

DNA and antibodies. The full-length Hec1 cDNA was subcloned into pEGFP-N1 containing a modified flexible linker region. Site-directed mutagenesis was performed to change Hec1 S165 into S165A or S165E, as well as to introduce a nonsense mutation rendering Hec1-GFP constructs RNAi-resistant. All constructs were validated by sequence analysis. Hec1-GFP constructs were subsequently subcloned into pQCXIP retroviral vector. Retroviral constructs and a plasmid expressing VSV-G were cotransfected into GP2 293 packaging cell line (Emi *et al.*, 1991; Burns *et al.*, 1993).

An antibody specific to phospho-residue of S165 of Hec1 was raised against the synthetic phosphopeptide CKRIFKDLGTPFAL(pS)KSS. Phospho-specific antibodies were obtained from a two-step affinity-purification process (first using the non-phospho-peptide affinity column, and then using the phospho-peptide column). To visualize Nek2, we preextracted cells for 1 min with 0.5% Triton X-100

in PGEM buffer (80 mM PIPES, pH 6.8, 5 mM EGTA, 1 mM $MgCl_2$, 4 M glycerol) and fixed them for 10 min with ice-cold methanol. Antibodies and their respective dilutions used for immunofluorescence staining or Western blotting were as follows: mouse monoclonal anti-Hec1 (9G3), mouse anti-BubR1, rabbit anti-ZW10, and rabbit anti-Zwint1 (GeneTex, Irvine, CA); rabbit anti-Mad1 (H-228; Santa Cruz Biotechnology, Santa Cruz, CA); mouse anti–α-tubulin (B-5-1-2; Sigma-Aldrich, St. Louis, MO); mouse anti-Nek2 (BD Transduction Laboratories, Franklin Lakes, NJ, and lab-made), mouse anti-GFP (Roche, Indianapolis, IN); rabbit anti-PP1α (GTX105255; GeneTex); rabbit anti-PP1γ (GTX105618; GeneTex); human ACA (Antibodies Incorporated, Davis, CA); and mouse anti-Mad2 (a gift from Anna Santamaria, University of Basel, Basel, Switzerland).

Immunoprecipitation. Protocol was adapted from Durfee *et al.* (1993). Briefly, aliquots were lysed in 500 µl lysis 250 buffer (50 mM Tris, pH 7.4, 250 mM NaCl, 5 mM ethylenediaminetetraacetic acid [EDTA], 5 mM ethylene glycol tetraacetic acid [EGTA], 0.1% Nonidet P-40, 50 mM NaF, 1 mM phenylmethylsulfonyl fluoride [PMSF], 1 mg/ml pepstatin A, 1 mg/ml aprotinin, 1 mg/ml leupeptin, 1 mg/ml antipain) and subjected to three liquid nitrogen freeze–thaw cycles. Lysate was clarified by centrifugation at 16,000 rpm for 2 min at room temperature. Clarified lysate was diluted to 125 mM NaCl. For immunoprecipitation, the lysate was incubated with antibodies at 4°C for 90 min, which was followed by Protein G Sepharose overnight. Immunoprecipitates were washed five times with wash buffer (50 mM Tris, pH 7.4, 125 mM NaCl, 5 mM EDTA, 5 mM EGTA, 0.1% Nonidet P-40, 50 mM NaF, and 1 mM PMSF). The lysate and immunoprecipitates were separated by SDS–PAGE, transferred to Immobilon-P membranes (Millipore, Billerica, MA), and subjected to immunoblot analysis.

Immunofluorescence staining and microscopy

Cells were grown on acid-etched coverslips and gently lysed with 0.5% Triton X-100 in PHEM Buffer (80 mM PIPES, 25 mM HEPES, pH 7.2, 10 mM EGTA, 4 mM $MgSO_4$) for 5 min and subsequently fixed for 20 min in PHEM buffer containing 4% paraformaldehyde (Electron Microscopy Sciences, Hatfield, PA; Wu *et al.*, 2009). Cells were blocked with 5% normal goat serum in PHEM, and then incubated with primary antibodies in phosphate-buffered saline overnight at 4°C. Secondary antibodies used were conjugated with Alexa Fluor 488, 546, or 633 (Molecular Probes, Invitrogen). When detecting Hec1 pS165, we added 500 nM Microcystin-LR (Alexis Biochemicals, San Diego, CA) to the lysis buffer. 4′,6-Diamidino-2-phenylindole (DAPI) staining was applied after secondary antibody incubation, and cells were finally mounted on microscope slides with ProLong Gold antifade reagent (Invitrogen). Static and time-lapse images were captured using a Carl Zeiss Axiovert 200M motorized, inverted microscope equipped with a Zeiss LSM 710 multispectral analyzer (Carl Zeiss, New York). Serial sections of cells were acquired and images were analyzed using Volocity (PerkinElmer, Waltham, MA). All image files were converted to TIFF, and Illustrator CS3 (Adobe, San Jose, CA) was used to assemble the figures. For time-lapse studies, cells were grown in glass bottom dishes (MatTek, Ashland, MA) and imaged within an enclosed temperature-, humidity-, and CO_2-controlled environment.

Quantification and statistical analysis

Measurement and quantification of kinetochore and microtubule intensities was done using ImageJ (http://rsb.info.nih.gov/ij). For quantifying kinetochore intensities, a circular region with fixed diameter was centered over the kinetochore and intensities were measured for both the protein of interest and, unless otherwise stated, for ACA. ACA was used for normalization after subtraction of background intensity. Data from all quantifications are reported as the mean ± SEM. Significance between groups of data was assessed by two-way analysis of variance or by unpaired Student's *t* test using Prism software (GraphPad, La Jolla, CA). Results were considered significant when $p < 0.05$.

ACKNOWLEDGMENTS

We thank Anna Santamaria, Nathaniel Gray, and Jennifer DeLuca for generously providing us with reagents; Yumay Chen, Guideng Li, and Ryon Graf for their help in this work; and Erin Goldblatt for critical reading of the manuscript. This work was made possible in part through access to the Optical Biology Core facility of the Developmental Biology Center at University of California–Irvine. R.W. was supported by a predoctoral fellowship from the DOD Congressionally Directed Medical Research Program in Breast Cancer and the University of California–Irvine Medical Scientist Training Program. This work is supported by a grant from the National Institutes of Health (CA-107568) to W.H.L.

REFERENCES

Alushin GM, Ramey VH, Pasqualato S, Ball DA, Grigorieff N, Musacchio A, Nogales E (2010). The Ndc80 kinetochore complex forms oligomeric arrays along microtubules. Nature 467, 805–810.

Brito DA, Rieder CL (2009). The ability to survive mitosis in the presence of microtubule poisons differs significantly between human nontransformed (RPE-1) and cancer (U2OS, HeLa) cells. Cell Motil Cytoskeleton 66, 437–447.

Buffin E, Lefebvre C, Huang J, Gagou ME, Karess RE (2005). Recruitment of Mad2 to the kinetochore requires the Rod/Zw10 complex. Curr Biol 15, 856–861.

Burds AA, Lutum AS, Sorger PK (2005). Generating chromosome instability through the simultaneous deletion of Mad2 and p53. Proc Natl Acad Sci USA 102, 11296–11301.

Burns JC, Friedmann T, Driever W, Burrascano M, Yee JK (1993). Vesicular stomatitis virus G glycoprotein pseudotyped retroviral vectors: concentration to very high titer and efficient gene transfer into mammalian and nonmammalian cells. Proc Natl Acad Sci USA 90, 8033–8037.

Campbell MS, Gorbsky GJ (1995). Microinjection of mitotic cells with the 3F3/2 anti-phosphoepitope antibody delays the onset of anaphase. J Cell Biol 129, 1195–1204.

Cheeseman IM, Chappie JS, Wilson-Kubalek EM, Desai A (2006). The conserved KMN network constitutes the core microtubule-binding site of the kinetochore. Cell 127, 983–997.

Chen Y, Riley DJ, Chen PL, Lee WH (1997). HEC, a novel nuclear protein rich in leucine heptad repeats specifically involved in mitosis. Mol Cell Biol 17, 6049–6056.

Chen Y, Riley DJ, Zheng L, Chen PL, Lee WH (2002). Phosphorylation of the mitotic regulator protein Hec1 by Nek2 kinase is essential for faithful chromosome segregation. J Biol Chem 277, 49408–49416.

Ciferri C *et al.* (2008). Implications for kinetochore-microtubule attachment from the structure of an engineered Ndc80 complex. Cell 133, 427–439.

DeLuca JG, Gall WE, Ciferri C, Cimini D, Musacchio A, Salmon ED (2006). Kinetochore microtubule dynamics and attachment stability are regulated by Hec1. Cell 127, 969–982.

DeLuca JG, Howell BJ, Canman JC, Hickey JM, Fang G, Salmon ED (2003). Nuf2 and Hec1 are required for retention of the checkpoint proteins Mad1 and Mad2 to kinetochores. Curr Biol 13, 2103–2109.

Diaz-Rodriguez E, Sotillo R, Schvartzman J, Benezra R (2008). Hec1 overexpression hyperactivates the mitotic checkpoint and induces tumor formation in vivo. Proc Natl Acad Sci USA 105, 16719–16724.

Du J *et al.* (2008). The mitotic checkpoint kinase NEK2A regulates kinetochore microtubule attachment stability. Oncogene 27, 4107–4114.

Durfee T, Becherer K, Chen PL, Yeh SH, Yang Y, Kilburn AE, Lee WH, Elledge SJ (1993). The retinoblastoma protein associates with the protein phosphatase type 1 catalytic subunit. Genes Dev 7, 555–569.

Elowe S, Hummer S, Uldschmid A, Li X, Nigg EA (2007). Tension-sensitive Plk1 phosphorylation on BubR1 regulates the stability of kinetochore microtubule interactions. Genes Dev 21, 2205–2219.

Emi N, Friedmann T, Yee JK (1991). Pseudotype formation of murine leukemia virus with the G protein of vesicular stomatitis virus. J Virol 65, 1202–1207.
Gentry MS, Hallberg RL (2002). Localization of *Saccharomyces cerevisiae* protein phosphatase 2A subunits throughout mitotic cell cycle. Mol Biol Cell 13, 3477–3492.
Glinsky GV, Berezovska O, Glinskii AB (2005). Microarray analysis identifies a death-from-cancer signature predicting therapy failure in patients with multiple types of cancer. J Clin Invest 115, 1503–1521.
Gorbsky GJ, Ricketts WA (1993). Differential expression of a phospho-epitope at the kinetochores of moving chromosomes. J Cell Biol 122, 1311–1321.
Guimaraes GJ, Dong Y, McEwen BF, Deluca JG (2008). Kinetochore-microtubule attachment relies on the disordered N-terminal tail domain of Hec1. Curr Biol 18, 1778–1784.
Hames RS, Fry AM (2002). Alternative splice variants of the human centrosome kinase Nek2 exhibit distinct patterns of expression in mitosis. Biochem J 361, 77–85.
Hames RS, Wattam SL, Yamano H, Bacchieri R, Fry AM (2001). APC/C-mediated destruction of the centrosomal kinase Nek2A occurs in early mitosis and depends upon a cyclin A-type D-box. EMBO J 20, 7117–7127.
Hayes MJ, Kimata Y, Wattam SL, Lindon C, Mao G, Yamano H, Fry AM (2006). Early mitotic degradation of Nek2A depends on Cdc20-independent interaction with the APC/C. Nat Cell Biol 8, 607–614.
Hayward DG, Fry AM. (2006). Nek2 kinase in chromosome instability and cancer. Cancer Lett 237, 155–166.
Helps NR, Luo X, Barker HM, Cohen PT (2000). NIMA-related kinase 2 (Nek2), a cell-cycle-regulated protein kinase localized to centrosomes, is complexed to protein phosphatase 1. Biochem J 349, 509–518.
Hewitt L, Tighe A, Santaguida S, White AM, Jones CD, Musacchio A, Green S, Taylor SS (2010). Sustained Mps1 activity is required in mitosis to recruit O-Mad2 to the Mad1-C-Mad2 core complex. J Cell Biol 190, 25–34.
Huang H, Hittle J, Zappacosta F, Annan RS, Hershko A, Yen TJ (2008). Phosphorylation sites in BubR1 that regulate kinetochore attachment, tension, and mitotic exit. J Cell Biol 183, 667–680.
Kemmler S, Stach M, Knapp M, Ortiz J, Pfannstiel J, Ruppert T, Lechner J (2009). Mimicking Ndc80 phosphorylation triggers spindle assembly checkpoint signalling. EMBO J 28, 1099–1110.
Kienitz A, Vogel C, Morales I, Muller R, Bastians H (2005). Partial downregulation of MAD1 causes spindle checkpoint inactivation and aneuploidy, but does not confer resistance towards taxol. Oncogene 24, 4301–4310.
Kim Y, Holland AJ, Lan W, Cleveland DW (2010). Aurora kinases and protein phosphatase 1 mediate chromosome congression through regulation of CENP-E. Cell 142, 444–455.
King RW, Deshaies RJ, Peters JM, Kirschner MW (1996). How proteolysis drives the cell cycle. Science 274, 1652–1659.
King RW, Peters JM, Tugendreich S, Rolfe M, Hieter P, Kirschner MW (1995). A 20S complex containing CDC27 and CDC16 catalyzes the mitosis-specific conjugation of ubiquitin to cyclin B. Cell 81, 279–288.
Kwiatkowski N *et al*. (2010). Small-molecule kinase inhibitors provide insight into Mps1 cell cycle function. Nat Chem Biol 6, 359–368.
Lin YT, Chen Y, Wu G, Lee WH (2006). Hec1 sequentially recruits Zwint-1 and ZW10 to kinetochores for faithful chromosome segregation and spindle checkpoint control. Oncogene 25, 6901–6914.
Liu D, Vleugel M, Backer CB, Hori T, Fukagawa T, Cheeseman IM, Lampson MA (2010). Regulated targeting of protein phosphatase 1 to the outer kinetochore by KNL1 opposes Aurora B kinase. J Cell Biol 188, 809–820.
Lou Y, Yao J, Zereshki A, Dou Z, Ahmed K, Wang H, Hu J, Wang Y, Yao X (2004). NEK2A interacts with MAD1 and possibly functions as a novel integrator of the spindle checkpoint signaling. J Biol Chem 279, 20049–20057.
Martin-Lluesma S, Stucke VM, Nigg EA (2002). Role of Hec1 in spindle checkpoint signaling and kinetochore recruitment of Mad1/Mad2. Science 297, 2267–2270.
Miller SA, Johnson ML, Stukenberg PT (2008). Kinetochore attachments require an interaction between unstructured tails on microtubules and Ndc80 (Hec1). Curr Biol 18, 1785–1791.
Musacchio A, Hardwick KG (2002). The spindle checkpoint: structural insights into dynamic signalling. Nat Rev Mol Cell Biol 3, 731–741.
Musacchio A, Salmon ED (2007). The spindle-assembly checkpoint in space and time. Nat Rev Mol Cell Biol 8, 379–393.
Nishino M, Kurasawa Y, Evans R, Lin SH, Brinkley BR, Yu-Lee LY (2006). NudC is required for Plk1 targeting to the kinetochore and chromosome congression. Curr Biol 16, 1414–1421.
O'Regan L, Blot J, Fry AM (2007). Mitotic regulation by NIMA-related kinases. Cell Div 2, 25.
Pinsky BA, Nelson CR, Biggins S (2009). Protein phosphatase 1 regulates exit from the spindle checkpoint in budding yeast. Curr Biol 19, 1182–1187.
Saurin AT, van der Waal MS, Medema RH, Lens SM, Kops GJ (2011). Aurora B potentiates Mps1 activation to ensure rapid checkpoint establishment at the onset of mitosis. Nat Commun 2, 316.
Sliedrecht T, Zhang C, Shokat KM, Kops GJ (2010). Chemical genetic inhibition of Mps1 in stable human cell lines reveals novel aspects of Mps1 function in mitosis. PLoS One 5, e10251.
Sudakin V, Ganoth D, Dahan A, Heller H, Hershko J, Luca FC, Ruderman JV, Hershko A (1995). The cyclosome, a large complex containing cyclin-selective ubiquitin ligase activity, targets cyclins for destruction at the end of mitosis. Mol Biol Cell 6, 185–197.
Tighe A, Staples O, Taylor S (2008). Mps1 kinase activity restrains anaphase during an unperturbed mitosis and targets Mad2 to kinetochores. J Cell Biol 181, 893–901.
Trinkle-Mulcahy L, Andersen J, Lam YW, Moorhead G, Mann M, Lamond AI (2006). Repo-Man recruits PP1 gamma to chromatin and is essential for cell viability. J Cell Biol 172, 679–692.
Uto K, Nakajo N, Sagata N (1999). Two structural variants of Nek2 kinase, termed Nek2A and Nek2B, are differentially expressed in *Xenopus* tissues and development. Dev Biol 208, 456–464.
Vanoosthuyse V, Hardwick KG (2009). A novel protein phosphatase 1-dependent spindle checkpoint silencing mechanism. Curr Biol 19, 1176–1181.
van 't Veer LJ *et al*. (2002). Gene expression profiling predicts clinical outcome of breast cancer. Nature 415, 530–536.
Waters JC, Chen RH, Murray AW, Gorbsky GJ, Salmon ED, Nicklas RB (1999). Mad2 binding by phosphorylated kinetochores links error detection and checkpoint action in mitosis. Curr Biol 9, 649–652.
Wong OK, Fang G (2007). Cdk1 phosphorylation of BubR1 controls spindle checkpoint arrest and Plk1-mediated formation of the 3F3/2 epitope. J Cell Biol 179, 611–617.
Wu G, Qiu XL, Zhou L, Zhu J, Chamberlin R, Lau J, Chen PL, Lee WH (2008). Small molecule targeting the Hec1/Nek2 mitotic pathway suppresses tumor cell growth in culture and in animal. Cancer Res 68, 8393–8399.
Wu G, Wei R, Cheng E, Ngo B, Lee WH (2009). Hec1 contributes to mitotic centrosomal microtubule growth for proper spindle assembly through interaction with Hice1. Mol Biol Cell 20, 4686–4695.